# Recent Developments in Tokamak Edge Physics Analysis at Garching

D.P. Coster 1), X. Bonnin 2), K. Borrass 1), H.-S. Bosch 1), B. Braams 3), H. Buerbaumer 4), A. Kallenbach 1), M. Kaufmann 1), J.-W. Kim 1), E. Kovaltsova 5), E. Mazzoli 6), J. Neuhauser 1), D. Reiter 7), V. Rozhansky 5), R. Schneider 2), W. Ullrich 1), S. Voskoboynikov 5), P. Xantopoulos 8) and the ASDEX Upgrade team 1)

1) Max-Planck-Institut für Plasmaphysik, EURATOM Association, 85748 Garching, Germany
2) Max-Planck-Institut für Plasmaphysik, EURATOM Association, 17489 Greifswald, Germany
3) Courant Institute, NYU, New York, USA
4) Institut für Allgemeine Physik, TU Wien, Austria, Association EURATOM-OEAW
5) St. Petersburg State Technical University, St. Petersburg, Russia
6) Politecnico di Torino, Italy
7) Düsseldorf University, Düsseldorf, Germany
8) N.C.S.R. 'Demokritos', GR-15310 A.G. Paraskevi, Greece

E-mail contact of main author: David.Coster@ipp.mpg.de

**Abstract.** The use of the SOLPS edge plasma and neutral codes is discussed. First SOLPS4.0 B2-Eirene is used to understand the role of C radiation in lowering the divertor target power load and the effects of power, density and divertor geometry on helium compression and enrichment. Then the newer B2-SOLPS5.0 is used in an interpretive mode to derive edge transport coefficients from experimental data, and then, with drift effects included, to model scrape-off layer currents. Finally some analytic and semi-analytic results are mentioned. The understanding of divertor power loading, helium compression and enrichment, edge transport coefficients and drifts are all important for current machines, but vital for extrapolation to future machines.

# 1 C Radiation

B2-Eirene [1,2] (the combination of two codes, a fluid plasma code (B2) [3,4] capable of treating multiple species and a Monte-Carlo neutrals code (Eirene) [5] capable of treating the detailed production and subsequent evolution of background and impurity neutrals) code runs together with a detailed experimental campaign have lead to a better understanding of the role of radiation in limiting peak fluxes to the target [6–8]. In these runs, and in similar runs for ITER [9–11], carbon radiation is observed to play an important role.

The importance of the C radiation can be understood in terms of a simple model relating the energy lost by C and D radiation to the C and D produced by D recycling. This produces a favourable feedback scenario regulating the radiation in the low plasma temperature divertor plasmas characteristic of partial detachment. However the problem of tritium co-deposition associated with carbon in a reactor device has re-opened the choice of materials for the divertor. It remains to be seen if the beneficial role played by carbon radiation can be entirely replaced by radiation from one (or perhaps a combination of) the noble gases.

## 2 He Compression

Also important for a reactor is the ability to exhaust the helium ash. An extensive series of runs [12] with the B2-Eirene code have been performed to explore the dependence of helium compression (the ratio of helium density at the pump to the midplane density close to the separatrix) and enrichment on plasma parameters and divertor configuration.

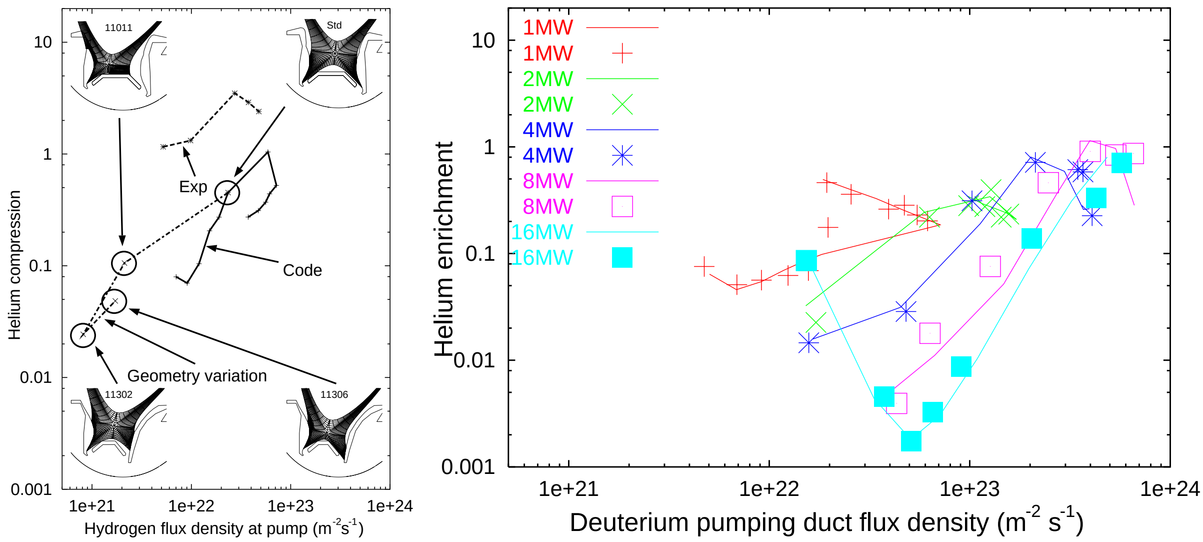


(a) (b)

Figure 1: (a) Helium compression from the experiment, from the code for a range of densities for one configuration and for 4 different configurations at a fixed density plotted versus hydrogen flux density at the pump duct entrance. (b) Data and fit for He enrichment.

As shown in figure 1(a), these results agree qualitatively with experimental results on ASDEX Upgrade [13, 14], though are somewhat too conservative quantitatively. The functional dependence of the D and He compression on the power crossing the separatrix into the Scrape-Off Layer, $P_{SOL}$, and the upstream separatrix electron density, $n_{e,sep}$, can be well approximated by a power law in the two quantities fitted separately for three regimes corresponding to the sheath limited regime, the high recycling regime and the detached regime. The transition between the regimes is based on a "break" density normalised to $n_{e,sep}$ and $P_{SOL}$.

$$F(n_{e,sep}, P_{SOL}, n_{e,break}, \lambda, S) = \exp(-(n_{e,sep}/(n_{e,break} * P_{SOL}^{\lambda}))^{S})$$

$$\begin{aligned} G(P_{SOL}, n_{e,sep}) = \; & F(n_{e,sep}, P_{SOL}, n_{e,sheath}, \lambda_{n_{e,sheath}}, S) * a^2 * P_{SOL}^{b} * n_{e,sep}^{c} \\ & +(1 - F(n_{e,sep}, P_{SOL}, n_{e,sheath}, \lambda_{n_{e,sheath}}, S)) \\ & *(F(n_{e,sep}, P_{SOL}, n_{e,detach}, \lambda_{n_{e,detach}}, S) * d^2 * P_{SOL}^{e} * n_{e,sep}^{f} \\ & +(1 - F(n_{e,sep}, P_{SOL}, n_{e,detach}, \lambda_{n_{e,detach}}, S)) * g^2 * P_{SOL}^{h} * n_{e,sep}^{i}) \end{aligned}$$

The coefficients in the fit are found by a non-linear regression based on the B2-Eirene results, and are given in table 1.

The resultant fit and data points from B2-Eirene is shown in figure 1(b).

| Regime | sheath | | high recycling | | detached | |
|---|---|---|---|---|---|---|
| Exponent for | $P_{SOL}$ | $n_{e,sep}$ | $P_{SOL}$ | $n_{e,sep}$ | $P_{SOL}$ | $n_{e,sep}$ |
| Deuterium | -0.129157 | **0.00** | -0.887993 | **1.0** | 1.88265 | **-2.00** |
| Helium | 1.36857 | **-4.00** | -4.55607 | 14.4873 | 1.46927 | **-1.0** |

Table 1: Table of coefficients fitted by non-linear regression to the simulation results of D and He compression. The bold-face coefficients were imposed and not fitted.

# 3 B2-SOLPS5.0

B2-Eirene has been extended to include the effects of drifts and currents. This is partly motivated by experimental evidence of differences observed when the toroidal field direction is changed, and partly by the wish to have as complete a set of physics as possible in the codes. An extensive programme was launched to re-derive the appropriate equations and then to implement them in a new version of the plasma code, B2.5 [15–18]. As expected the neoclassical results are recovered on the closed field line region. This work is being further extended to include additional terms in the potential equation thus improving the model for the radial electric field, and to properly account for drift effects on impurities. As an example of the use of the new code, we show in figure 2 measurements of the current at the outer target plate of ASDEX Upgrade, as well as early results from simulations. Another example can be found in [19].

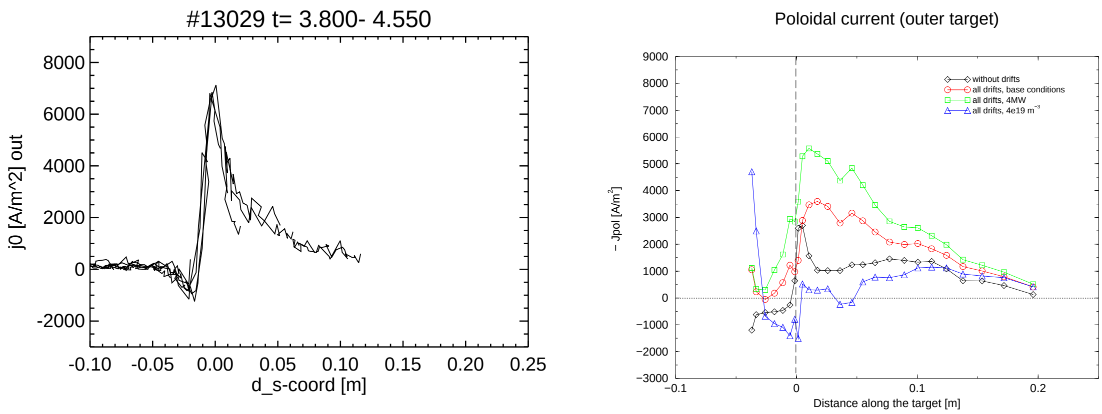


Figure 2: Experimental and calculated target electric currents at the outer target plate of ASDEX Upgrade.

## 3.1 Interpretive Version

Using the fluid neutral model in the new B2.5 code, an interpretive version of the code has been prepared. Mid-plane density and temperature profiles, as well as other experimental data, are used to derive the underlying transport coefficients by a non-linear fitting procedure [20, 21] with a residual given by

$$\alpha_1 \frac{1}{M} \sum_M G_{T_e} \left( \frac{T_e^{exp} - T_e^{code}}{\Delta T_e^{exp}} \right)^2 + \alpha_2 \frac{1}{N} \sum_N G_{n_e} \left( \frac{n_e^{exp} - n_e^{code}}{\Delta n_e^{exp}} \right)^2$$

$$+\alpha_3 \frac{1}{N} \sum_N G_{\nabla n_e} \left( \frac{\nabla n_e^{exp} - \nabla n_e^{code}}{\Delta \nabla n_e^{exp}} \right)^2 + \alpha_4 \left( \frac{\Gamma_{pump}^{exp} - \Gamma_{pump}^{code}}{\Delta \Gamma_{pump}^{exp}} \right)^2 + \alpha_5 \left( \frac{\Gamma_{wall}^{exp} - \Gamma_{wall}^{code}}{\Delta \Gamma_{wall}^{exp}} \right)^2$$

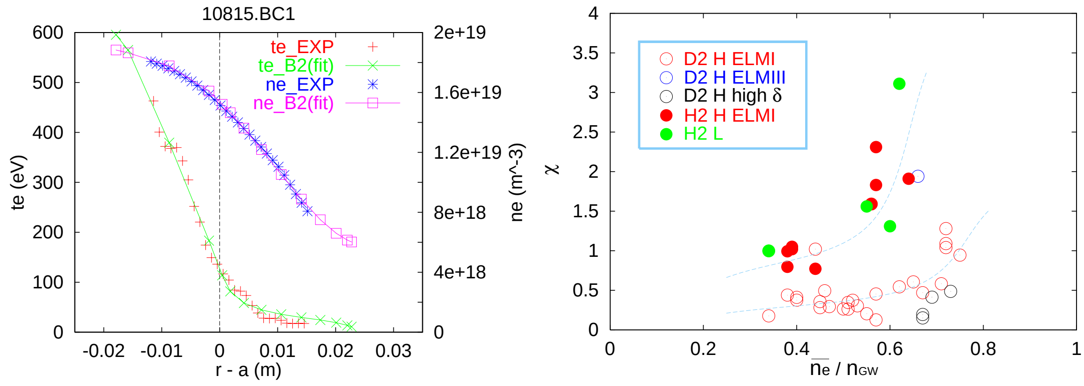


(a) (b)

Figure 3: (a) Example of a fit from the code to the experimental data. (b) Thermal diffusivity versus the density normalized to Greenwald density.

and the fitted quantities, $D$, $\chi$, $n_{e,core}$, $c_{pump}$ and the separatrix position are varied to minimise this residual.

Figure 3(b) shows $\chi$ versus a normalized density derived from a set of ELMy H-mode ASDEX Upgrade shots where a suggestive increase in transport is seen close to the Greenwald density limit.

A regression analysis can then be performed on resultant $D$ and $\chi$ to find their dependencies on plasma and engineering parameters.

$$\begin{aligned} \chi &\propto I_p{}^{-1.32\pm0.26} B_t{}^{-0.60\pm0.39} P_{sol}{}^{0.93\pm0.12} \bar{n}_e{}^{0.50\pm0.26} m_{eff}{}^{-1.57\pm0.27} \\ D &\propto I_p{}^{-0.90\pm0.24} P_{sol}{}^{0.48\pm0.14} m_{eff}{}^{-0.41\pm0.32} \end{aligned}$$

where $I_p$ is the plasma current, $B_t$ the toroidal field, $P_{sol}$ the power crossing the separatrix, $\bar{n}_e$ the line average density and $m_{eff} \equiv \frac{m_D \bar{n_D} + m_H \bar{n_H}}{m_p(\bar{n_D} + \bar{n_H})}$ the average atomic mass number.

In order to facilitate the future implementation of mesh refinement in the code, the earlier treatment for the momentum equation by using a staggered grid for the velocities has been replaced by a cell centred treatment. The modifications for the mesh refinement are well under way.

Semi-empirical models have been used to investigate the interrelation between SOL and pedestal in low frequency ELMing H-modes. Experimental findings on density and temperature profiles in the pedestal and near separatrix SOL regions are combined with information provided by analytical SOL models to derive relations among various combinations of pedestal and SOL quantities. The approach has been successful in describing the separatrix to pedestal density ratio in ASDEX Upgrade [22,23] and the scaling of the low pressure boundary of Type-I H-mode cycles in JET [24].

A previously proposed edge density limit model [25,26] has been extended to include the isotope dependence and was successfully tested against L-mode density limit data from JET H, D and T discharges [27].

Diverging findings are reported from experiment, computational studies and analytical considerations as regards the ratio $\lambda_n/\lambda_T$ ($\lambda_n$ and $\lambda_T$ the upstream density and temperature fall-off lengths, respectively) and a possible correlation between the two. An extensive study has been launched to clarify to what extend these discrepancies can be resolved within the context of standard edge transport models. This effort includes numerical as well as analytical elements.

# References


[1] SCHNEIDER, R. et al., J. Nucl. Mater. **196–198** (1992) 810.

[2] REITER, D., J. Nucl. Mater. **196-198** (1992) 80.

[3] BRAAMS, B. J., *Computational Studies in Tokamak Equilibrium and Transport*, PhD thesis, Rijksuniversiteit, Utrecht, Nederland., 1986.

[4] BRAAMS, B. J., A multi-fluid code for simulation of the edge plasma in tokamaks, Technical Report 68, Next European Torus, 1987.

[5] REITER, D. et al., J. Nucl. Mater. **220–222** (1995) 987, PSI 94 Mito.

[6] KALLENBACH, A. et al., Nucl. Fusion **39** (1999) 901.

[7] COSTER, D. P. et al., Czech. Journ. of Phys. **48** (1998) 327.

[8] COSTER, D. P. et al., Towards a better understanding of power loading and carbon radiation in the divertor, in *Europhysics Conference Abstracts (CD-ROM), Proc. of the 26th EPS Conference on Controlled Fusion and Plasma Physics, Maastricht, 1999*, edited by BASTIAN, C. et al., volume 23J, pages 1517–1520, Geneva, 1999, EPS.

[9] KUKUSHKIN, A. et al., Analysis of ITER divertor performance and ITER tokamak edge parameter database, in *Plasma Physics and Controlled Nuclear Fusion Research 1996*, volume 2, pages 987–993, Vienna, 1997, IAEA.

[10] KUKUSHKIN, A. S. et al., Contrib. Plasma Phys. **38** (1998) 20.

[11] KUKUSHKIN, A. S. et al., Divertor performance in reduced-Technical-Objective/Reduced-Cost ITER, in *Europhysics Conference Abstracts (CD-ROM), Proc. of the 26th EPS Conference on Controlled Fusion and Plasma Physics, Maastricht, 1999*, edited by BASTIAN, C. et al., volume 23J, pages 1545–1548, Geneva, 1999, EPS.

[12] COSTER, D., B2-Eirene modelling of helium compression and enrichment, submitted to Journal of Nuclear Materials.

[13] BOSCH, H.-S. et al., J. Nucl. Mater. **266–269** (1999) 462.

[14] BOSCH, H.-S., Helium transport and exhaust with an ITER-like divertor in ASDEX Upgrade, submitted to Journal of Nuclear Materials.

[15] BRAAMS, B. et al., Contrib. Plasma Phys. **36** (1996) 276.

[16] ROZHANSKY, V. et al., Modeling of self-consistent electric fields in tokamak edge plasma with b2.5 code, in *Europhysics Conference Abstracts (CD-ROM), Proc. of the 26th EPS Conference on Controlled Fusion and Plasma Physics, Maastricht, 1999*, edited by BASTIAN, C. et al., volume 23J, pages 1749–1752, Geneva, 1999, EPS.

[17] SCHNEIDER, R. et al., Contrib. Plasma Phys. **40** (2000) 328.

[18] ROZHANSKY, V. et al., Contrib. Plasma Phys. **40** (2000) 423.

[19] ROZHANSKY, V. et al., Modeling of tokamak edge plasma for discharges with neutral beam injection, submitted to Journal of Nuclear Materials.

[20] COSTER, D. et al., Contrib. Plasma Phys. **40** (2000) 334.

[21] KIM, J.-W., ASDEX Ugpgrade edge transport scalings from the 2-dim interpretation code B2.5-I, submitted to Journal of Nuclear Materials.

[22] BORRASS, K. et al., Nucl. Fusion **39** (1999) 843.

[23] SCHWEINZER, J. et al., Separatrix to pedestal density ratio in ASDEX Upgrade H-modes comparing DIV-I and DIV-II operation, in *Europhysics Conference Abstracts (CD-ROM), Proc. of the 26th EPS Conference on Controlled Fusion and Plasma Physics, Maastricht, 1999*, edited by BASTIAN, C. et al., volume 23J, pages 1525–1528, Geneva, 1999, EPS.

[24] LINGERTAT, J. et al., Characterisation of elm triggered edge pressure cycles in JET, in *Europhysics Conference Abstracts (CD-ROM), Proc. of the 26th EPS Conference on Controlled Fusion and Plasma Physics, Maastricht, 1999*, edited by BASTIAN, C. et al., volume 23J, page 261, Geneva, 1999, EPS.

[25] BORRASS, K. et al., Nucl. Fusion **37** (1997) 523.

[26] BORRASS, K. et al., Contrib. Plasma Phys. **38** (1998) 130.

[27] MAGGI, C. F. et al., Nucl. Fusion **39** (1999) 979.